LA-UR 93 - 2305

Los Alamos National Laboratory is operated by the University of California for the United States Department of Energy under contract W-7405-ENG-36

TITLE THE APPLICATION OF FRONT TRACKING TO THE SIMULATION OF SHOCK REFRACTIONS AND SHOCK ACCELERATED INTERFACE MIXING

AUTHOR(S) D. H. Sharp, T-13
J.W. Grove, SUNY
Y. Yang, US DOE
Q. Zhang, National Science Foundation Grant
J. Glimm, Institute of Cornell University
B. Boston, US DOE
R. Holmes, US DOE

SUBMITTED TO The Proceedings of the 4th International Workshop on the Physics of Compressible Turbulent Mixing.

DISCLAIMER

Los Alamos Los Alamos National Laboratory
Los Alamos, New Mexico 87545

THE APPLICATION OF FRONT TRACKING TO THE SIMULATION OF SHOCK REFRACTIONS AND SHOCK ACCELERATED INTERFACE MIXING

JOHN W. GROVE[1,2,3,5], YUMIN YANG[4], QIANG ZHANG[4,6], DAVID H. SHARP[7], JAMES GLIMM[1,2,3,4], BRIAN BOSTON, AND RICHARD HOLMES

ABSTRACT. We report new results on the Rayleigh Taylor and Richtmyer-Meshkov instabilities. Highlights include calculations of Richtmyer-Meshkov instabilities in curved geometries without grid orientation effects, improved agreement between computations and experiments in the case of Richtmyer-Meshkov instabilities at a plane interface, and a demonstration of an increase in the Rayleigh-Taylor mixing layer growth rate with increasing compressibility, along with a loss of universality of this growth rate. The principal computational tool used in obtaining these results was a code based on the front tracking method

1. INTRODUCTION

The mixing behavior of two or more fluids plays an important role in a number of physical processes and technological applications. We consider two basic types of mechanical (*i.e.*, non diffusive) fluid mixing. If a heavy fluid is suspended above a lighter fluid in the presence of a gravitational field, small perturbations at the fluid interface will grow. This process is known as the Rayleigh-Taylor instability. One can visualize this instability in terms of bubbles of the light fluid rising into the heavy fluid, and fingers (spikes) of the heavy fluid falling into the light fluid. A similar process, called the Richtmyer Meshkov instability [13, 15], occurs when an interface is accelerated by a shock wave. These instabilities have several common features. Indeed, Richtmyer's approach to understanding the shock induced instability was to view that process as resulting from an acceleration of the two fluids by a strong gravitational field acting for a short time.

We examine three separate aspects of the Rayleigh Taylor and Richtmyer Meshkov problems. Section 2 discusses direct numerical simulations of Richtmyer Meshkov type problems using front tracking. Front tracking is an adaptive method which provides sharp resolution of distinct waves in fluid flows. This is accomplished by the use of a dynamically moving co dimension one grid that follows the tracked wave fronts. Our conclusion is that front tracking is a valuable numerical method due to its ability to remove numerical diffusion, enhance the resolution of the computation, and reduce or eliminate grid orientation effects. Section 3 describes an analysis of the short term growth in the unstable modes of a shocked interface using a linearization of the Euler equations.

1991 *Mathematics Subject Classification* 35L67 76L05

Key words and phrases Rayleigh Taylor, Richtmyer Meshkov, front tracking

[1]Supported in part by the U.S. Army Research Office through the Mathematical Sciences Institute of Cornell University under subcontract to SUNY Stony Brook, ARO contract number DAAL03 91 C 0027

[2]Supported in part by the National Science Foundation Grant no. DMS 9201584

[3]Supported in part by the U.S. Army Research Office, grant no. DAAL03 92 G 0185

[4]Supported in part by the Applied Mathematics Subprogram of the U.S. Department of Energy DE FG02 90ER25084

[5]Supported in part by the National Science Foundation Grant no. DMS 9057129

[6]Supported in part by the Oak Ridge National Laboratory subcontract 19X SJ067V

[7]Supported by U.S. Department of Energy

We compare the solution of the linearized equations with an impulsive model of the mixing process due to Richtmyer, and with numerical solutions of the full Euler equations. We show that for sufficiently small amplitudes of the perturbations in the fluid interface, the linear theory agrees with the numerical solutions to the fully nonlinear system. We noticed that in many cases the results of the impulsive model disagreed with the exact solution to the linearized equations. We also report in section 4 on recent work that has examined the role of compressibility in the Rayleigh-Taylor problem. It is shown that the mixing layer growth rate increases markedly with increasing compressibility and this effect is accompanied by a loss of universality. This is the first prediction of an important property of the Rayleigh-Taylor mixing layer outside of the range of existing experiments.

2. Front Tracking Simulations of Shock Induced Surface Instabilities

The front tracking method represents a surface of discontinuity in a fluid flow as a sharp interface, thereby eliminating numerical diffusion. This results in a substantial increase in computational resolution, and a corresponding increase in efficiency, which has been utilized to increase the detail and scope of computations attempted. Moreover, front tracking can be combined with modern shock capturing methods to provide a computational tool of great flexibility for modeling flows dominated by shocks and fluid interfaces. The shock capturing provides a robust alternative to tracking when the interacting waves produce configurations that are too complicated to track, while tracking improves the ability of the shock capturing code to resolve secondary features of the flow. The general goal of our effort is to achieve a good balance between the increased resolution of the tracked wave fronts and the robustness of the shock capturing methods.

An important aspect of our front tracking code in simulations of the Richtmyer Meshkov instability is its ability to handle interactions between tracked waves. It can automatically detect the collision of two wave fronts, analyze the resulting interaction, and modify the tracked wave data structures accordingly. References [4, 6, 9, 11, 12] describe the basic algorithms and provide details on the construction of our front tracking code.

Figure 1 shows a front tracking simulation of the acceleration of a perturbed circular interface by an expanding shock wave. The computation begins with a bubble of heavy fluid suspended in a lighter fluid. The two fluids are initially at rest, and the bubble interface is given a slight sinusoidal perturbation of the form $r = (r_0 + \epsilon \cos(n\theta))$, where (r, θ) are the polar coordinates of a point on the bubble interface. Here $r_0 = 0.8$, $\epsilon = 0.05$, and $n = 12$. Both fluids are modeled using a polytropic equation of state with $\gamma = 1.33$, and the density ratio across the bubble is 5. An expanding shock with ahead Mach number 6.6 (pressure ratio 50) is installed at a distance 0.3 from the origin. The entire computation takes place within a square of side 6.0 using a 200×200 grid.

At about time 0.19 the expanding shock reaches the bubble interface and is refracted into an inwardly directed rarefaction wave, and an outwardly directed transmitted shock. Note that we track both edges of the reflected rarefaction. Figure 1b shows the tracked wave configuration shortly after the expanding shock has passed through the bubble interface. By this point the average radius of the bubble interface is approximately twice its initial value and the ripples on the interface have experienced a phase inversion. Such an inversion is typical for interactions that produce reflected rarefactions.

Figure 1c shows the simulation just before the leading edge of the reflected rarefaction reaches the origin. The reflection of the rarefaction wave at the origin produces additional outwardly directed waves. These new waves are not tracked in our simulation, but are still reasonably well resolved by the shock capturing method.

Figure 1d shows the later time development of the bubble interface. Here the spikes of the heavy fluid being ejected into the lighter fluid outside have become quite elongated. We also see that the heads of the fingers are starting to pinch off. The velocity shear across the sides of the fingers is

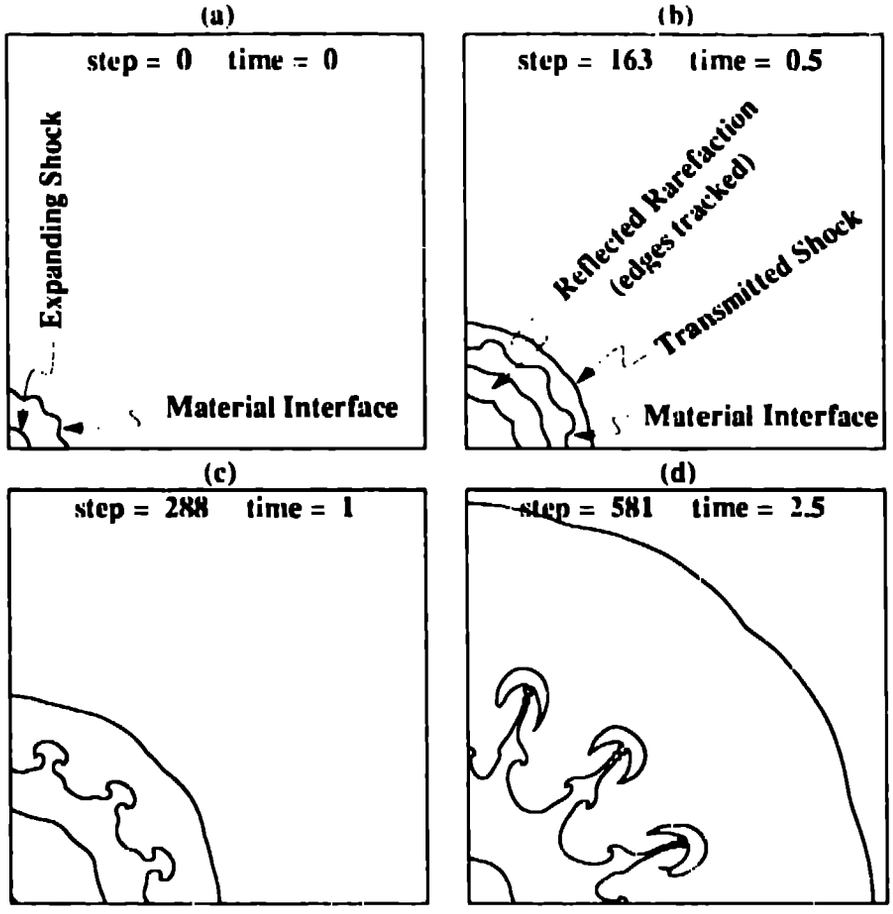

FIGURE 1. The acceleration of a perturbed circular interface by a shock wave. A significant advantage of front tracking is the improvement in the resolution of interface features not aligned with the finite difference grid. Note that even at late times the three fingers have nearly the same shape and extension.

substantial, which explains the production of the Kelvin Helmholtz type roll up on the sides of the fingers.

This computation illustrates several important points. First is the ability of front tracking to reduce grid orientation effects on the fluid interface. Since the underlying rectangular grid is square, the effective grid size in directions diagonal to the grid is $\sqrt{2}$ times coarser than in directions parallel to the grid. Unless the grid is quite fine, this can produce a substantial degradation in the resolution of waves in these directions. This effect was cited, for example, in [1, 5] to explain the relatively faster growth of fingers aligned with the coordinate axes as compared to fingers oriented at oblique angles to the grid. We emphasize that there is very little indication of grid orientation effect in our computation. Since the initial data is periodic in θ with period $\pi/6$, each of the three spikes in figure 1 should be identical. In our simulation we see that there is only about a 2.5% difference in the elongation of the spikes at the latest time shown.

We also comment that the asymmetry in the Kelvin Helmholtz roll up on the sides of the outer spikes appears to be due to an additional artificial mode that has been produced by the interaction of the tracked wave with the boundary. For efficiency we conducted these simulations using a quarter circular geometry with the axes of symmetry along the positive x and y axes replaced by reflecting boundaries. As implemented, this results in a slight loss of information at the boundaries, and can lead to the development of additional modes in such highly unstable problems as this one. We are currently investigating improved algorithms for the propagation of curves at reflecting walls

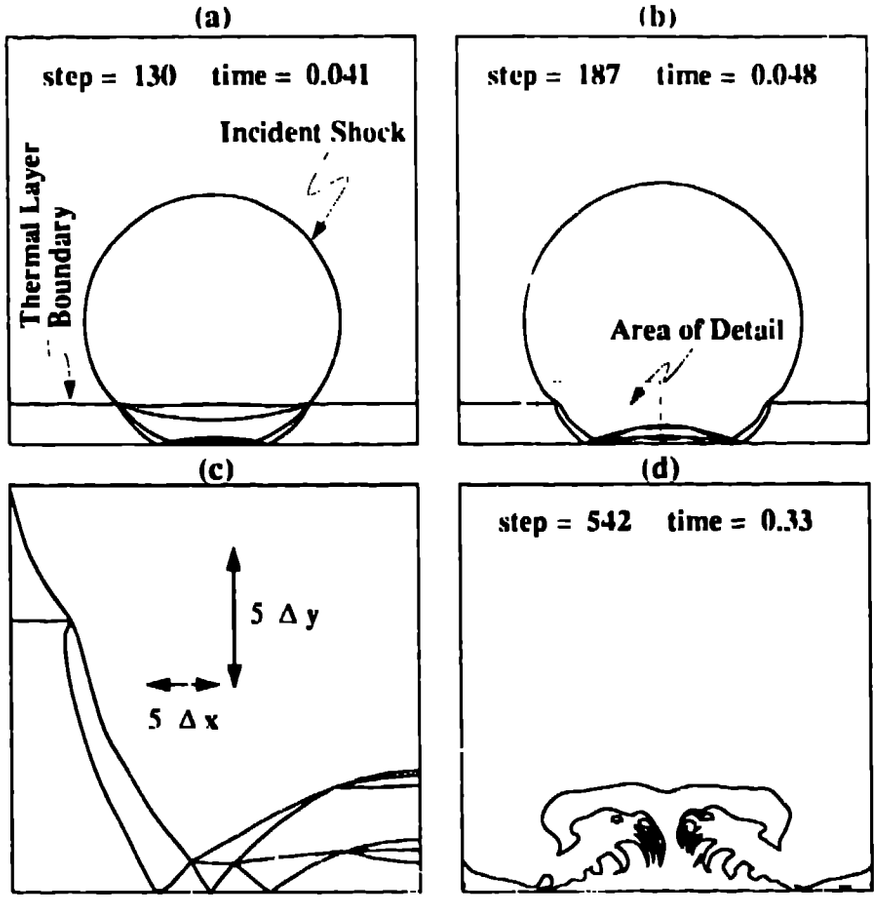

FIGURE 2. The interaction of a shock wave with a thermal boundary layer. Figures 2a-b show the early stages of the simulation which is dominated by multiple wave interactions. Figure 2c shows a detail from (b) illustrating the complexity of the tracked waves. Note that here the y coordinate has been scaled by a factor of two to improve the visibility of the multiple wave interactions. Figure 2d shows the late time formation of a central geyser in the layer.

which we hope will eliminate this extra mode.

Finally we observe that the expanding nature of the outgoing shock wave has an effect on the fluid interface quite similar to that of a gravitational acceleration which enhances the unstable behavior of the interface.

Figures 2 show a simulation of the acceleration of a thermal boundary layer by an expanding shock wave. Such a layer might, for example, be produced by radiant energy from the explosion that initiates the shock wave. This computation illustrate two important points. The first is the ability of the front tracking code to handle complex interactions between the tracked waves. The second is that a sharp resolution of these features is absolutely essential for obtaining the correct answer to the questions of interest here.

The layer is modeled as a region of warm gas bounded by the wall and a contact discontinuity. A circular, expanding shock wave is initiated at a distance from the wall of three times the width of the thermal layer, and an initial radius of half the thermal layer width. The fluid outside the shock is at rest, and the density ratio between the gas inside and outside the thermal layer is 0.5. An adiabatic exponent of $\gamma = 1.1$ is used for the equation of state. The pressure ratio across the shock is initially 10^5, which gives an initial shock Mach number of 92.6. The collision between the shock and thermal layer produces a number of interesting wave interactions and bifurcations that

are all installed and handled automatically by our code.

When the incident shock hits the thermal layer, it produces a pair of connected shock refractions with reflected rarefactions. As the blast continues to expand, there is eventually a bifurcation in the structure of the two dimensional wave pattern created by the refraction of the blast wave through the thermal layer boundary. When this happens, the transmitted wave outruns the incident wave producing a precursor type configuration as described in [10]. In modeling this bifurcation we track the precursor shock and the original incident shock but not the reflected rarefactions. This explains the absence of the two middle wave edges between figures 2a and 2b, which only show the tracked waves in the simulation. This rarefaction is still present in the computation as a captured wave.

Figure 2c shows a detail from figure 2b of the reflection of the tracked waves near the wall. The expanding nature of these waves leads to an eventual bifurcation from a regular to a Mach type reflection that has been installed for the outermost pair of reflections in figure 2c. The thermal layer acts like a channel for the waves inside it leading to a series of multiple reflections. All of this complicated structure is resolved within a zone of only about 20×10 grid blocks. Eventually the dominant characteristics of the flow shift from wave interactions to chaotic mixing, and at some point we cease tracking all of the waves except the thermal boundary interface. Figure 2d shows the interface at late time.

3. The Richtmyer Meshkov instability in Plane Geometry

The extremely complex nature of the Richtmyer Meshkov instability makes it essential to investigate simplified fluid configurations that can be used to interpret experiments and to validate numerical computations. We analyze here the case where a plane fluid interface at rest is accelerated by the passage of a single plane shock wave through the interface.

If we represent the interface position at time t by $y(x) = a(t)\cos kx$, a formula for the amplitude growth rate, $\dot{a}(t)$, was conjectured by Richtmyer [15] as

$$\dot{a}(t) = ku\frac{\rho_+ - \rho_-}{\rho_+ + \rho_-}a(0+) \tag{3.1}$$

where u is the average velocity of the contact surface after the interaction, ρ_+ and ρ_- are the post shocked densities on the two sides of the contact, and $a(0+)$ is the perturbation amplitude immediately after the shock-contact interaction.

Formula (3.1), called the impulsive model, is based on the assumption that the main effect of the shock wave passing through the interface is to compress the fluids on either side of the interface and to give the fluid near the interface a push. It is also assumed that once the shock has passed through the interface the fluids are incompressible. Richtmyer verified his conjecture using a linearization of the Euler equations, and he demonstrated agreement between the impulsive model and the solution of the linearized equations for a small parameter range corresponding to the case of a reflected shock.

As a first step in our program we solved the linear equations numerically for a much broader range of parameters, including both the case of reflected shocks and rarefactions. Illustrative results are given in table 1. Our units are chosen such that $U_s = \rho_a = k = 1$, where U_s is the speed of incident shock, ρ_a is the density of the state ahead of the incident shock, and k is the perturbation wave vector. We can also set $a(0-)$ to one since in the linear theory the growth rate, $\dot{a}(t)$, is proportional to this pre shocked perturbation amplitude. The solution of the linearized equations is completely determined by four dimensionless parameters: the adiabatic exponents γ_1 and γ_2, the pre shocked desity ratio ρ_1/ρ_2, and the incident shock strength $(p_b - p_a)/p_b$. The subscripts 1 and 2 refer quantities on the incident and transmitted side of the fluid interface respectively, and a and b refer to the ahead and behind sides of the incident shock. For the reflected shock case we points of agreement as well as disagreement between the impulsive model and the linear theory. The reflected rarefaction case showed substantial disagreement between the two theories.

Table 1a
Reflected Shock

	1.1	2.0	4.0	8.0	16.0
1.0	0.0052	0.019	0.11	0.16	0.18
	0.011	0.080	0.14	0.18	0.18
0.5	0.011	0.070	0.11	0.12	0.11
	0.013	0.080	0.12	0.13	0.11
0.05	0.0015	0.0090	0.013	0.013	0.012
	0.0015	0.0092	0.013	0.014	0.012

(a)

Table 1b
Reflected Rarefaction

	0.91	0.5	0.25	0.125	0.0625
1.0	0.0044	-0.014	-0.025	-0.12	-0.26
	0.0042	0.028	-0.048	-0.059	-0.061
0.5	-0.011	-0.081	-0.15	-0.19	0.21
	0.0068	-0.047	-0.077	-0.086	-0.080
0.05	-0.0016	-0.013	-0.026	-0.037	-0.045
	-0.00078	-0.0054	-0.088	-0.0099	-0.0093

(b)

TABLE 1. Comparison of terminal velocities between the impulsive model and linear theory. The left column of table 1a shows the incident shock strength $[(p_b - p_a)/p_b]$, and the top row the pre-shocked density ratio (ρ_1/ρ_2). The upper number in each entry is from the impulsive model, and the lower is the result of numerical simulations of the linear theory The two adiabatic exponents are $\gamma_1 = \gamma_2 = 1.5$.

We have also compared the results of the linear theory to those obtained by simulation of the full Euler equations. This serves both to determine the range of validity of the linear theory and to validate the solution of the full Euler equations at small amplitudes.

Figures 3 and 4 show a comparison of the linear theory and the full Euler equations. In this problem the interface is accelerated by a shock moving from air to SF_6. The parameters were chosen to agree with those occurring in the experiments reported by Benjamin [2]. The density ratio of SF_6 to air at standard conditions is 5.1, and the adiabatic exponents were taken as $\gamma_{air} = 1.4$ and $\gamma_{SF_6} = 1.0394$. The initial amplitude, $a(0-)$, was 0.0637 times the period of the sinusoidal perturbation. Figure 3 shows a plot of the normalized amplitude of the fluid interface, $a(t)/a(0-)$, after its acceleration by a shock with ahead Mach number $M_0 = 1.24$. Figure 4 shows the value of $\dot{a}(t)/a(0-)$ for the same simulation together with the value calculated from the Benjamin's experiments [2]. The horizontal time axis in these figures is normalized so that $t = 0$ corresponds to the time at which the shock wave has completed its refraction through the interface.

Referring to the figures we emphasize the following points. First, for sufficiently small amplitudes the simulations of the linear theory and the full Euler equations agree. Second, the growth rate as determined by the solution of the full Euler equations is in substantial agreement with the experimentally measured growth rate. Third, the growth rate as predicted by the linear theory, which agrees with the impulsive model in this case, disagrees with experiment by a factor of approximately two.

In these figure we also compare front tracking calculations where all curves were tracked (incident, reflected and transmitted shock waves and material interface) and where only the material interface is tracked. We note that while the two nonlinear computations agree for much of the simulation they begin to diverge at late times.

In ongoing work we are investigating the case of reflected rarefactions, the effects of mass diffusion on the mixing rates, and exploring the interaction over a wide range of flow parameters.

4. THE INFLUENCE OF COMPRESSIBILITY ON THE GROWTH RATE OF A RAYLEIGH TAYLOR MIXING LAYER

Previous investigations [7, 8, 16] reported on the behavior of the outer envelope of the bubbles produced by a Rayleigh Taylor unstable interface. For incompressible or nearly incompressible flows, the height of this envelope is given by

$$h(t) = \alpha A g t^2, \tag{4.1}$$

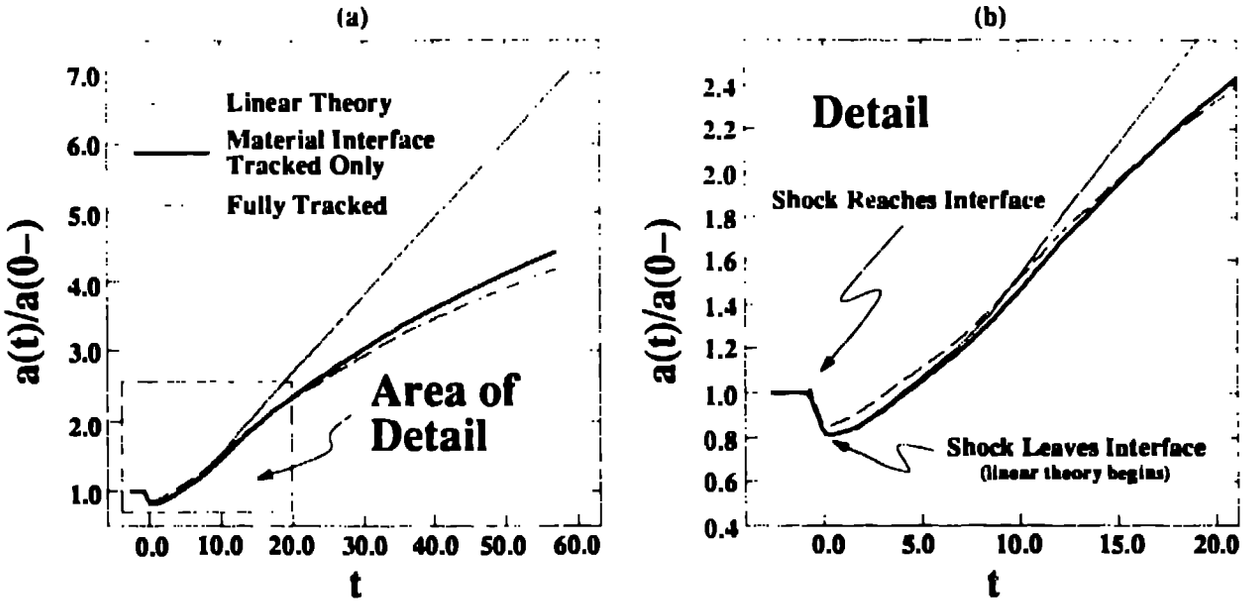

FIGURE 3. A comparison of three separate calculations of the amplitude, $a(t)/a(0-)$, of a shocked air-SF_6 interface. We see that the linear theory agrees with the nonlinear computations for sufficiently small amplitudes. Figure 3b shows a detail for early times in the computations.

where $A = (\rho_2 - \rho_1)/(\rho_2 + \rho_1)$ is the Atwood ratio of the densities of the two fluids, g is the gravitational acceleration, and $\alpha \approx 0.06$ is an approximately universal constant. We use $M^2 = \lambda g/c_h^2$ as a dimensionless measure of the compressibility, where λ is the wave length of the perturbation, and c_h^2 is the sound speed of the heavy fluid at the interface. The number α is universal in the sense that it is independent of both the thermodynamic properties of the two fluids, as well as the initial conditions at the unstable interface. This formula agrees with the experimental results of Read and Youngs [14].

Further justification of the validity of formula (4.1) was provided by analysis which established the existence of a renormalization group fixed point for a set of equations that approximate the fluid motion in terms of the dynamics of a statistical ensemble of elementary modes governed by pairwise interactions [8, 16]. Numerical solutions of this model gave a value for α in excellent agreement with both experiments and computations.

The above investigations, which were conducted for compressibilities $M^2 \leq 0.1$, have been extended to flows with moderate to large values of M^2. We conducted a series of numerical simulations of Rayleigh-Taylor unstable flows for a variety of different parameter regimes and values of M^2 ranging from 0.1 to 1.0 [3]. Two significant observations were made on the basis of these numerical computations. The first is that α shows a marked dependence on M^2, with the value of α for $M^2 = 1$ nearly two and a half times the value of the incompressible ($M^2 = 0$) limit of $\alpha_{incomp} = 0.06$. In general, α appears to an increasing function of M^2. The second observation was that α was no longer universal for larger values of M^2, which is expressed by a dependence of α on the initial distribution of the perturbations on the unstable interface.

Table 2a summarizes the results of our investigation into the dependence of α on compressibility. The value of α, as summarized in the last column of table 2a, was computed by fitting the bubble height $h(t)$, as measured from an ensemble of N different numerical simulations, versus t^2. Each individual simulation used a different set of random surface perturbations to act as seeds for the unstable modes, and the reported value of α is the statistical average of the individual α_i's of the separate runs. For sample runs with $N > 1$ the root mean square (rms) is also reported. The other

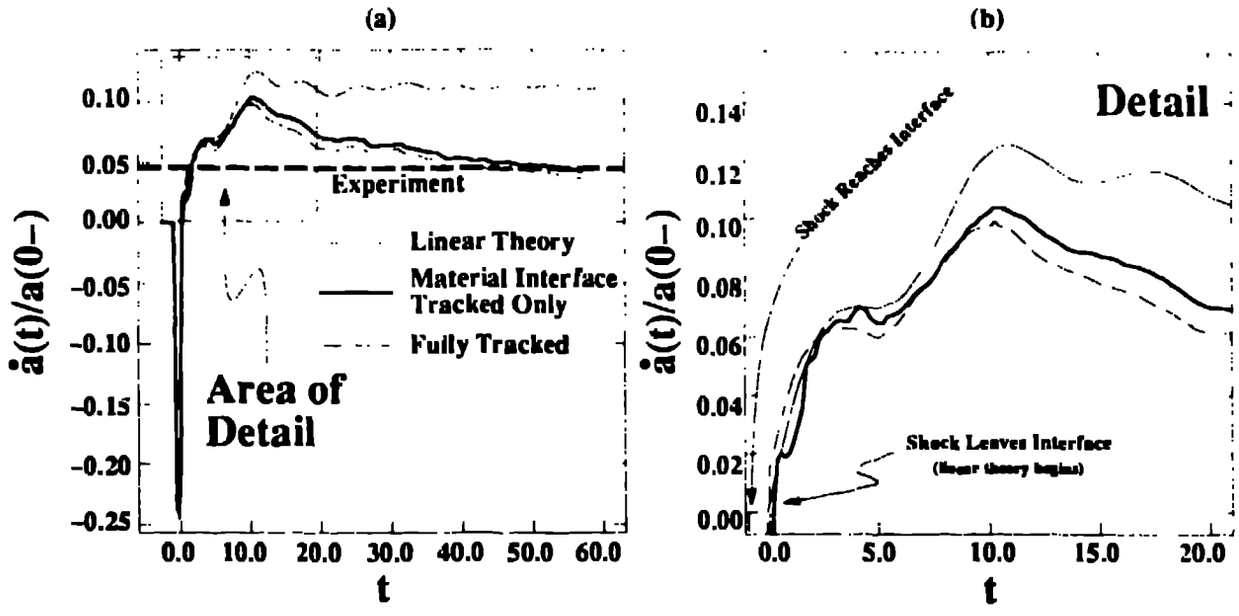

FIGURE 4. The rate of change, $\dot{a}(t)$, of the amplitude of a shocked air-SF_6 interface. The dark dashed line shows the measurement of $\dot{a}(t)/a(0-)$ obtained from the experiments of Benjamin [2] using the same flow parameters as used in this computation. The experimental number has been converted into dimensionless units as mentioned in the text.

columns of table 2 report respectively, the compressibility M^2 of the initial configuration, the grid sizes used for the simulation, the minimum and maximum of the fourier modes used to generate the initial random interface, the number of fourier modes ($k_{max} - k_{min} + 1$), and the number N of samples. In each sample, the amplitudes of the fourier modes were selected from independent Gaussian random variables.

The data reported in table 2a clearly indicate an increase in α for larger values of M^2. We also note that for $M^2 = 0.5$, α is also dependent on the number of modes on the initial random surface.

We also compared the predicted values of α as computed from the renormalization group fixed point model with the numerical computations. These results are summarized in table 2b. We observe a dependence of α on M^2, and note that the RG fixed point model begins to fail for larger values of M^2.

5. Conclusion

This article summarizes recent work by members of our group on the modeling and analysis of unstable fluid interfaces. Our experience is that front tracking is an effective tool for the computation of these flows in two dimensions and allows us to achieve good resolution of complex flows even on relatively coarse grids.

To summarize, our principal conclusions are: front tracking substantially reduces grid orientation effects for computations in curved geometries, the solution of the linearized Euler equations agrees with numerical solutions of the full Euler equations for the Richtmyer Meshkov problem at sufficiently small amplitudes, our front tracking simulation of the Richtmyer-Meshkov problem agrees with the experimental results of Benjamin, and the rate of growth of a Rayleigh Taylor mixing layer increases with increasing compressibility.

Table 2a
The growth rate α for a Rayleigh-Taylor mixing layer

Line	M^2	Domain	k_{max}	k_{min}	Modes	Samples	Modulation	α
1	.1	208 × 300	36	24	13	1	Yes	.062
2		208 × 300	18	6	13	1	Yes	059
3		208 × 300	22	10	13	1	Yes	.066 ± .004
4		208 × 300	22	10	13	8	No	068 ± .004
5		640 × 300	78	39	40	1	Yes	.072
6	.2	320 × 300	37	18	20	4	No	.084 ± .003
7	.3	320 × 300	37	18	20	4	No	096 ± .004
8	.5	104 × 300	10	5	6	1	Yes	.0736
9		104 × 300	10	5	6	8	No	099 ± .008
10		320 × 300	37	18	20	1	Yes	105
11		320 × 300	37	18	20	8	No	.121 ± .006
12		320 × 300	28	9	20	1	Yes	.106
13		320 × 300	57	38	20	1	Yes	.106
14		640 × 300	74	35	40	1	Yes	119
15		960 × 300	114	55	65	1	Yes	.123
16		1280 × 300	159	80	80	1	Yes	.116
17	1	640 × 300	74	35	40	1	Yes	.137
18		960 × 300	114	55	65	1	Yes	.144

Table 2b
A comparsion of α to RG Theory

M^2	α_{comp}	α_{model}	error (%)
0.1	0.062 0.070	0.064-0.076	0
0 2	0.081-0.087	0.073-0.080	1
0.3	0 092-0.100	0 080-0 086	7
0 5	0.114-0.128	0.089 0.094	19
1.0	0.137-0.144	0.105-0.107	24

TABLE 2. Table 2a shows the results of our numerical computations of the growth ra for a Rayleigh-Taylor mixing layer. A Comparison of α as predicted by numerical simulatio vs. the renormalization group theory is shown in table 2b This table is reproduced from reference [3].

ACKNOWLEDGMENTS

We wish to thank the other members of the front tracking group at the University at Stony Brook for their assistance in this project. In particular we thank Y. Deng, and Y. Chen who were two of the main contributors to the numerical computations discussed in section 4. Use of the Intel iPSC/860 located at Oak Ridge National Laboratory and NASA Ames is also gratefully acknowledged.

REFERENCES

1 D Arnett, B Fryxell, and E Muller, *Instabilities and nonradial motion in SN 1987a*, Astrophysical J 341 (1989), L63 L66

2 R Benjamin, *Experimental observations of shock stability and shock induced turbulence*, Advances in Compressible Turbulent Mixing (5285 Port Royal Rd Springfield VA 22161) (W P Dannevik, A C Buckingham, and C E Leith, eds), National Technical Information Service, U S Department of Commerce, 5285 Port Royal Rd Springfield VA 22161, 1992, pp 341 348

3. Y. Chen, Y. Deng, J. Glimm, G. Li, D. H. Sharp, and Q. Zhang, *A renormalization group scaling analysis for compressible two-phase flow*, Phys. Fluids A, 1993, to appear.
4. I-L. Chern, J. Glimm, O. McBryan, B. Plohr, and S. Yaniv, *Front tracking for gas dynamics*, J. Comput. Phys. **62** (1986), 83–110.
5. B. Fryxell, E. Müller, and D. Arnett, *Instability and clumping in SN 1987a. I. early evolution in two dimensions*, The Astrophysical Journal **367** (1991), 619–634.
6. J. Glimm, J. Grove, W. B. Lindquist, O. McBryan, and G. Tryggvason, *The bifurcation of tracked scalar waves*, SIAM J. Comput. **9** (1988), 61–79.
7. J. Glimm, X. L. Li, R. Menikoff, D. H. Sharp, and Q. Zhang, *A numerical study of bubble interactions in Rayleigh-Taylor instability for compressible fluids*, Phys. Fluids A **2** (1990), no. 11, 2046–2054.
8. J. Glimm and D. H. Sharp, *Chaotic mixing as a renormalization group fixed point*, Phys. Rev. Lett. **64** (1990), 2137–21
9. J. Grove, *The interaction of shock waves with fluid interfaces*, Adv. Appl. Math. **10** (1989), 201–227.
10. ———, *A survey of the analysis of irregular shock refractions and its application to front tracking methods*, Proceedings of the Second Workshop on Hyperbolic Waves, Rio de Janeiro, Brazil, 1992.
11. ———, *Applications of front tracking to the simulation of shock refractions and unstable mixing*, J. Appl. Num. Math., to appear 1993, Proceedings of the U.S. Army Workshop on Adaptive Methods for Partial Differential Equations, ed. J. Flaherty, Rensselaer Polytechnic Institute, Troy, New York.
12. J. Grove and R. Menikoff, *The anomalous reflection of a shock wave at a material interface*, J. Fluid Mech. **219** (1990), 313–336.
13. E. E. Meshkov, *Instability of a shock wave accelerated interface between two gases*, NASA Tech. Trans. **F-13** (1970), 074.
14. K. I. Read, *Experimental investigation of turbulent mixing by Rayleigh-Taylor instability*, Physica D **12** (1984), 45.
15. R. D. Richtmyer, *Taylor instability in shock acceleration of compressible fluids*, Comm. Pure Appl. Math **13** (1960), 297–319.
16. Q. Zhang, *Validation of the chaotic mixing renormalization group fixed point*, Phys. Lett. A **151** (1990), 18–22.

Department of Applied Mathematics and Statistics, State University of New York at Stony Brook, Stony Brook, NY 11794-3600

E-mail address: glimm@ams.sunysb.edu, grove@ams.sunysb.edu, ymy@ams.sunysb.edu,, zhang@ams.sunysb.edu, boston@ams.sunysb.edu, holmes@ams.sunysb.edu

Complex Systems Group, Theoretical Division, Los Alamos National Laboratory, Los Alamos, NM 87545

E-mail address: dhs@t13.lanl.gov